Desalination and Water Treatment
www.deswater.com

1944-3994/1944-3986 © 2012 Desalination Publications. All rights reserved
doi: 10.1080/19443994.2012.698813

48 (2012) 199–206
October

Decolourization of C.I. Reactive Orange 16 via photocatalysis involving TiO_2/UV and TiO_2/UV/oxidant systems

Ozlem Esen Kartal*, Gulistan Deniz Turhan

Department of Chemical Engineering, Inonu University, Malatya, 44280 Turkey
Tel. +90 422 3774751; email: ozlem.kartal@inonu.edu.tr

Received 24 September 2011; Accepted 12 April 2012

ABSTRACT

Decolourization of C.I. Reactive Orange 16 (RO16) via photocatalysis involving TiO_2/UV and TiO_2/UV/oxidant systems has been investigated. The experiments were carried out in a stirred cylindrical batch photoreactor under UV irradiation. The effects of pH, TiO_2 concentration and addition of electron acceptors such as H_2O_2, $Na_2S_2O_8$ and Cu^+ ions were studied. The decolourization efficiency followed the order of pH 3 > pH 9 > pH 6 in TiO_2/UV system. The addition of Cu^+ ions to TiO_2/UV/oxidant system significantly increased the decolourization efficiency. The performance of addition of 0.5 mM Cu^+ ions to TiO_2/UV/$Na_2S_2O_8$ system was also evaluated by using synthetic dye-bath effluent. The results reveal that almost complete decolourization (99%) was achieved with RO16, while 76% decolourization was obtained with synthetic dye-bath effluent after 360 min of reaction time. Similar trend was observed with COD measurements. The rate of decolourization of RO16 was found to follow pseudo-first order kinetics and obeys L–H model. When the suspension of TiO_2 containing RO16 was exposed to solar irradiation, 90% of decolourization and 64% of COD removal were obtained after 120 min of reaction time. Degradation products of RO16 were determined by LCMS.

Keywords: Reactive Orange 16; TiO_2/UV; Decolourization; $Na_2S_2O_8$; Cu^+ ions; Hydroxyl radicals

1. Introduction

Reactive dyes are widely used in textile industry to dye cotton, wool and polyamide fibers, due to their properties such as simple application procedure, good stability during washing and bright colours. It has been estimated that 50% of reactive dyes are lost in dyeing processes as a result of a low dye–fiber fixation rate in comparison with other dyes and existence of unreactive hydrolyzed dye occurred via reaction of dye molecules with water [1]. Azo dyes, characterized by the presence of –N=N– azo bond linking aromatic rings, constitute one of the largest groups of reactive dyes. The release of them into environment is detrimental to the aquatic life, resulting receiving water bodies to become highly coloured and toxic. Apart from being aesthetically unpleasant, colour in natural water bodies decreases light penetration and photosynthesis [2,3]. Various conventional physical and chemical treatment technologies have been developed for the removal of azo dyes from textile effluents so far, but they are found to be ineffective or involved further treatments [4–6]. In addition, conventional aerobic biological treatment has also become difficult in oxidizing them because of their complicated non-biodegradable structure [7]. Aromatic amines which are more toxic, mutagenic and carcinogenic than dye molecules are also formed as intermediates in anaerobic conditions by reductive cleavage of

---

*Corresponding author.

azo bond [8,9]. Environmental concerns on water pollution involve considering more effective treatment technologies to eliminate intense colour from textile effluent, thus being able to meet the discharge standards.

In recent years, a promising remediation process as an alternative to conventional methods, the so-called Advanced Oxidation Processes (AOPs) was developed. AOPs have the potential to oxidize a wide range of water soluble organic pollutants via generation of highly reactive and non-selective hydroxyl radicals ($OH^{\bullet}$) as a strong oxidant with a standard redox potential of 2.8 V. These processes largely fall into the categories of semiconductor-assisted photocatalysis [10–18], ozonation [19,20], H_2O_2/UV photolysis [21,22] and Fenton and photo-Fenton type reactions [23–26] and successfully eliminate azo dyes. Among them, photocatalysis with TiO_2 has been extensively investigated because of its characteristics such as non-toxicity, chemically stability, low cost and possibility of using sunlight.

It is well established that, when TiO_2 suspension is irradiated with light energy equal or larger than the band gap energy, i.e. $h\nu \geq E_g = 3.2$ eV, an electron from the valance band is promoted to conduction band (e_{CB}^-), leaving a hole (h_{VB}^+) in the valance band. The photogenerated e_{CB}^- and h_{VB}^+ pair can either recombine or interact with surface species to initiate the subsequent redox reactions on the TiO_2 surface. The photogenerated holes react with $OH^{\bullet}$ and H_2O adsorbed or close to the surface to form $OH^{\bullet}$ radicals or oxidize the organic molecules directly. Upon reaction of the photogenerated electrons with O_2 adsorbed on the surface or dissolved which prevents its recombination with holes, superoxide radical anion ($O_2^{\bullet -}$) is formed [27–29]. Sequence of reactions on the surface of TiO_2 can be expressed as follows:

$$TiO_2 \xrightarrow{h\nu} TiO_2\left(e_{CB}^- + h_{VB}^+\right) \quad (1)$$

$$TiO_2(h_{VB}^+) + H_2O \rightarrow TiO_2 + OH^{\bullet} + H^+ \quad (2)$$

$$TiO_2(h_{VB}^+) + OH^- \rightarrow TiO_2 + OH^{\bullet} \quad (3)$$

$$TiO_2(e_{CB}^-) + O_2 \rightarrow TiO_2 + O_2^{\bullet -} \quad (4)$$

In the past three decades, TiO_2 based photocatalysis has proven to be effective for degradation or mineralization of organic contaminants in polluted water. Photocatalysis with TiO_2 is recognized with its potential either to mineralize non-biodegradable organic compounds completely into inorganic substances such as CO_2 and H_2O or to degrade them to biodegradable products under mild operating conditions. Thus, it can be applied alone or in combination with other treatment technologies as a pre-treatment step. TiO_2/UV system has been extensively applied for elimination of dyes from coloured textile wastewater. Juang et al. [30] studied the photodegradation of binary azo dyes in the presence of TiO_2 particles under UV irradiation. They reported that pH had a vital effect on removal of dyes and photodegradation of Acid Orange 7 and Reactive Red 2 in binary solutions was slower than in single dye solution. Mahmoodi et al. [31] investigated the photocatalytic degradation of Astrason Blue FGGL and Solophenyl Yellow FFL dyes by using immobilized TiO_2 particles and their results indicated that the photocatalytic decolourization of these dyes can be simulated by computational fluid dynamics modelling.

In an attempt to increase the decolourization efficiency of azo dyes, TiO_2/UV studies have been moved to TiO_2/UV/oxidant by adding electron acceptors such as H_2O_2 and $S_2O_8^{2-}$ ions to TiO_2/UV system. Yu et al. [32] studied the decolourization of C.I. Reactive Black 5 in UV/TiO_2, UV/oxidant and UV/TiO_2/oxidant systems and found that decolourization rate constant values followed the order $NaIO_4 > Na_2S_2O_8 > NaBrO_3 > H_2O_2 >$ absence of oxidant. Soutsas et al. [33] reported that the decolourization and degradation of four reactive dyes by photocatalytic processes depend on system parameters such as pH, TiO_2 loading, dye concentration and addition and concentration of H_2O_2. Addition of H_2O_2 at pH = 3 promoted the decolourization of Remazol Red RR.

Although several studies have been conducted for photo degradation of dyes at different operating conditions, it can be still beneficial to investigate in detail by considering addition of oxidants. Therefore, the objective of this study was to investigate the decolourization of C.I. Reactive Orange 16 (RO16) which is one of the most used reactive dyes for dyeing of cotton and silk in Turkey via photocatalysis involving TiO_2/UV and TiO_2/UV/oxidant systems. As shown in Fig. 1, it has an azo group contributing the colour and vinyl sulfone as the reactive group. After determining the best operating condition with RO16, we examined the decolourization of synthetic dye-bath effluent.

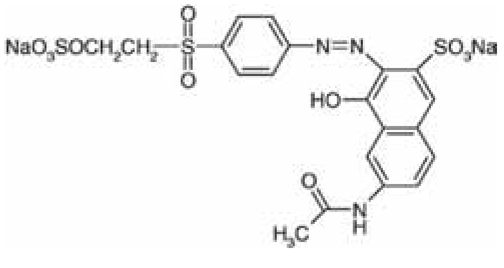

Fig. 1. Structure of C.I. Reactive Orange 16 (λ_{max} = 493 nm, M_w =617.54).

2. Experimental

2.1. Materials

A commercially available RO16 from DyStar was used as received and its chemical structure is given in Fig. 1. A gift sample of TiO_2-P25 having an average particle size of 21 nm and BET specific surface area of 50 m^2 g^{-1} was obtained from Degussa. It is mostly in anatase form. NaOH (Sigma) and H_2SO_4 (96% w/w, Merck) were used for pH adjustment. All chemicals were of analytical grade and used without further purification.

2.2. Experimental procedure

The decolourization of RO16 was carried out in a cylindrical batch photoreactor made up of a pyrexglass. The top of it was open to the atmosphere and equipped with a water jacket to maintain the temperature at 20 ± 2 °C. The photoreactor was surrounded by 4 UV-A lamps of 6 W (Topbulb) with a wavelength of 352 nm. The photoreactor and UV lamps were placed in a chamber covered by aluminium foil. The reaction mixture was vigorously stirred by means of magnetic stirrer during the experiments. The system was bubbled with oxygen through a glass circular distributor placed at the bottom of the reactor. The pH of the solution was adjusted by using either dilute NaOH or H_2SO_4 solutions and measured by a digital pH-meter (Hanna pH-221). The batch experiments were performed by using 2 L R016 solution of appropriate concentrations prepared with distilled water. After addition of TiO_2 to dye solution, the suspension was constantly stirred for 30 min in dark to attain equilibrium. Then the UV light turned on to initiate the reaction. Samples of 10 mL taken at regular time intervals were centrifuged at 4000 rpm for 30 min and filtered through a 0.2 μm cellulose acetate membrane filter to separate TiO_2 particles.

Solar experiment was performed between 12:00 and 14:00 h on a sunny day in May at Inonu University in Malatya (38°19′E, 38°21′N), Turkey. The total intensity reaching the suspension was measured by using a radiometer (Vilber Lourmat VLX-3W) equipped with a sensor operating in 365 nm.

In the case of using synthetic dye-bath effluent, the solution of RO16 was prepared by dissolving 2 g of RO16 in 1 L water heated at 80 °C. According to a dye-bath recipe, a mixture of 20 mL RO16 solution, 0.5 g L^{-1} enzyme, 0.5 g L^{-1} sequestering agent, 28 mL 30% w/w NaCl solution, 10 mL 20% w/w $NaCO_3$ solution and 34 mL water was prepared for cotton dyeing. After dyeing process, the obtained effluent was used as a synthetic dye-bath effluent in photocatalytic experiment.

In an attempt to identify the degradation products of RO16, LCMS analyses were conducted by means of Agilent 1100 LCMS using a capillary column of ACE 5 C18(4.6 μm × 250 mm) after 2 h of degradation.

2.3. Analysis

The decolourization of RO16 was evaluated by monitoring the dye concentration at maximum wavelength of 493 nm by means of Shimadzu UV-1700 Pharmaspec UV–Visible Spectrophotometer. The decolourization efficiency (η) of the samples was calculated from the equation given below

$$\eta(\%) = \frac{C_0 - C}{C_0} \times 100 \tag{5}$$

where C_0 and C are the initial and treated dye concentrations, respectively.

COD of the samples was determined with commercially available test kits (Matriks) by oxidation of samples with K_2CrO_7 in H_2SO_4 and heating for 2 h at 421 K in a COD reactor (Lovibond ET 108). Then, COD measurements were conducted by using a photometer (Lovibond PC Multidirect). Per cent COD removal of the samples were calculated from the equation given below:

$$COD(\%) = \frac{COD_0 - COD}{COD_0} \times 100 \tag{6}$$

where COD_o: COD at $t = 0$
COD: COD at $t = t$.

3. Results and discussion

3.1. Effect of pH

pH of suspension is an important parameter on photocatalytic degradation of dyes since it determines the surface charge of TiO_2 as well as the adsorption behaviour of the dyes. The point of zero charge of TiO_2 is at pH 6.8, therefore below this pH the surface is positively charged and above that it is opposite [7,34]. The effect of different pH levels on the decolourization of RO16 is presented in Fig. 2. RO16 has two sulfonate groups (SO_3^-) having negative charges in an aqueous solution in its chemical structure. Hence, in acidic media, electrostatic interactions between TiO_2 surface and dye anions favour the adsorption which results in high decolourization efficiency. In alkaline media, both TiO_2 surface and RO16 are negatively charged. Consequently, a weak adsorption onto the TiO_2 surface due to Coulombic repulsion between negatively charged TiO_2 surface and RO16 molecules leads to a decrease in decolourization efficiency. The effect of pH on decolourization efficiency

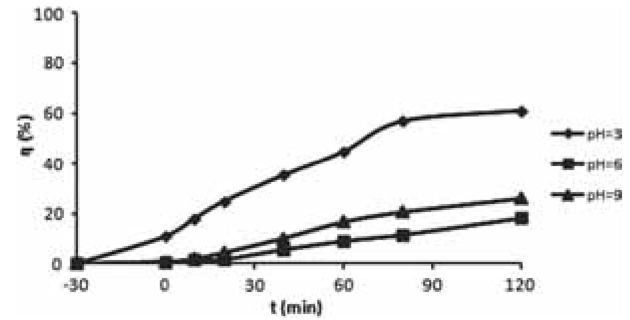

Fig. 2. Effect of pH on decolourization efficiency of RO16. $[TiO_2] = 2$ g L^{-1}, $[RO16] = 8.096 \times 10^{-2}$ mM

was investigated in a range of 3–9. As shown in Fig. 2, at pH = 3 surface adsorption is more effective (11%) than that of at pH values of 6 and 9 for the above-mentioned reasons. Besides as expected, the highest degree of decolourization efficiency (61%) was obtained at pH = 3. Alkaline medium gave relatively better decolourization than pH = 6 medium. In spite of a Coulombic repulsion between negatively charged TiO_2 surface and hydroxide ions, this can be attributed to that in alkaline medium $OH^\bullet$ radicals could be generated easily due to the presence of more available hydroxide ions [35]. Therefore, decolourization efficiency followed the order of pH 3 > pH 9 > pH 6.

3.2. *Effect of TiO_2 concentration*

The effect of TiO_2 concentration on the course of decolourization of RO16 was investigated in the range of 0.25–2 g L^{-1} with 8.096×10^{-2} mM RO16 concentration at suspension pH = 3 under UV irradiation. In the present study, 11% of RO16 adsorbed on TiO_2 surface after 30 min of equilibration time at the highest loading of catalyst (i.e. 2 g L^{-1}). As can be deduced from Fig. 3, decolourization efficiency seems to increase with increasing TiO_2 loading in the range studied. An appreciable decolourization was not observed in the absence of TiO_2 (i.e. direct photolysis) and loading of 2 g L^{-1} TiO_2 yielded 61% decolourization efficiency after 120 min reaction time. This is because availability of active sites on TiO_2 surface is increased with increase in catalyst concentration. It should be pointed out that, the amount of TiO_2 affects both a number of active sites on TiO_2 and the penetration of UV light through the suspension. As the amount of TiO_2 increases, a number of active sites increases, but the penetration of UV light into the suspension decreases due to shielding effect. Besides, particle agglomeration can occur at high catalyst concentration, decreasing surface area for light absorption and dye adsorption [7].

3.3. *Effect of added electron acceptors*

Electron acceptors promote the decolourization efficiency of dyes by inhibiting the recombination of photogenerated electron–hole pairs in the reaction [10]. Besides, avoiding recombination, they have some other effects such as generating more radicals and oxidizing species, increasing oxidation of intermediates and hindering deficiency occurred in the case of low O_2 concentration [36]. In this study, the effect of addition of electron acceptors such as H_2O_2 and $S_2O_8^{2-}$ ions for decolourization of RO16 under UV radiation was investigated.

Fig. 4 represents the effect of addition of 15 mM H_2O_2 as a function of pH of suspension. In acidic and neutral media, decolourization efficiency of RO16 was increased from 61% to 64% and from 18% to 35%, respectively, by adding H_2O_2 which traps photogenerated electrons through the following equation:

$$H_2O_2 + e^- \rightarrow OH^- + OH^\bullet \tag{7}$$

Also, since H_2O_2 is a powerful oxidant, it produces two $OH_\bullet$ under UV irradiation.

$$H_2O_2 + h\nu \rightarrow OH^\bullet + OH^\bullet \tag{8}$$

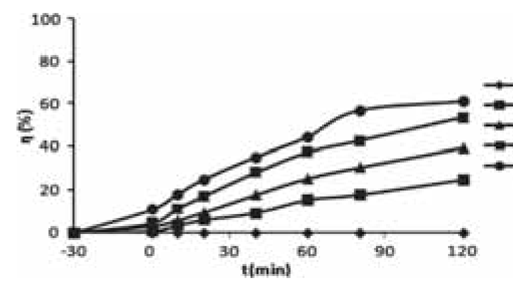

Fig. 3. Effect of TiO_2 concentration on decolourization efficiency of RO16. pH = 3, $[RO16] = 8.096 \times 10^{-2}$ mM.

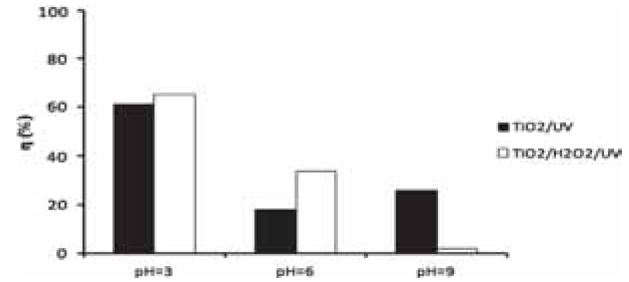

Fig. 4. Effect of H_2O_2 as a fuction of pH on decolourization efficiency of RO16. $[TiO_2] = 2$ g L^{-1}, $[RO16] = 8.096 \times 10^{-2}$ mM.

Accordingly, decolourization efficiency of RO16 was enhanced in the presence of H_2O_2 at acidic and neutral conditions. However, no observable decolourization of dye was obtained under alkaline conditions in which H_2O_2 decomposes to oxygen and water rather than forming $OH^{\cdot}$ (Eq. (9)) [37]

$$2H_2O_2 + h\nu \rightarrow 2H_2O + O_2 \tag{9}$$

As can be seen from Fig. 5, persulphate ions did not accelerate the decolourization but the addition of 0.5 mM Cu^+ ions to $TiO_2/UV/Na_2S_2O_8$ system improved the decolourization efficiency from 62% to 96% after 120 min of reaction time. The enhanced decolourization can be attributed to the production of additional sulfate radicals which is described by Eqs. (10)–(13) [17].

$$Cu^+ + S_2O_8^{2-} \rightarrow CuS_2O_8^- \tag{10}$$

$$CuS_2O_8– \rightarrow Cu^{2+} + SO_4^{2-} + SO_4^{-\bullet} \tag{11}$$

$$Cu^+ + SO_4^{-\bullet} \rightarrow Cu^{2+} + SO_4^{2-} \tag{12}$$

$$Cu^{2+} + S_2O_8^{2-} \rightarrow Cu^{3+} + SO_4^{2-} + SO_4^{-\bullet} \tag{13}$$

Similarly, addition of Cu^+ ions to $TiO_2/UV/H_2O_2$ system significantly increased the decolourization efficiency from 64% to 88% at reaction time of 120 min according to following equation [17]:

$$Cu^+ + H_2O_2 \rightarrow Cu^{2+} + OH^\bullet + OH^- \tag{14}$$

This can be explained that Cu^+ ions oxidized by H_2O_2 to Cu^{2+}, yielding additional $OH^\bullet$.

The performance of addition of 0.5 mM Cu^+ ions to $TiO_2/UV/Na_2S_2O_8$ system was also evaluated by using synthetic dye-bath effluent. Fig. 6 shows that almost complete decolourization (99%) was achieved with RO16, while 76% decolourization was obtained with synthetic dye-bath effluent after 360 min of reaction time. Similar trend was observed with COD measurements, indicating the evaluation of oxidative mineralization of the process. As can be seen in Table 1, 77% and 57% of COD removal levels were reached for RO16 and synthetic dye-bath effluent at the end of 360 min, respectively. Since auxiliary chemicals are used in dyeing process, synthetic dye-bath effluent contains a considerable amount of ions such as CO_3^- and Cl^- which lowers the photocatalytic activity by scavenging $OH^{\cdot}$ radicals [38]. Therefore, as expected both decolourization and COD removal values of synthetic dye-bath effluent were lower than those of RO16. Comparing COD removal levels to decolourization, mineralization was found lower than decolourization, indicating that a residual amount of organic load, composed of oxidation by-products, is remained in the treated suspension. From the point of view of achieving complete mineralization, it is important to have a longer irradiation time.

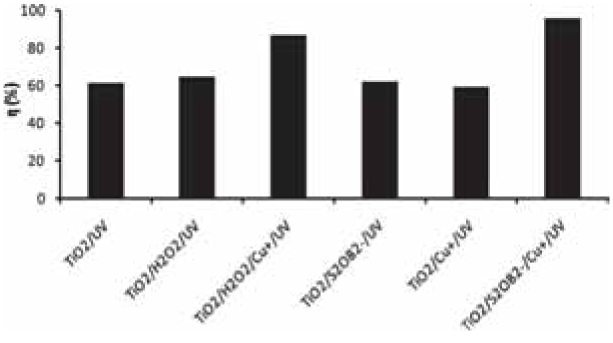

Fig. 5. Effect of oxidants on decolarization efficiency of RO16 at pH = 3, $[TiO_2]$= 2 g L^{-1}, [RO16] = 8.096 × 10^{-2} mM.

3.4. RO16 decolourization kinetics

In the literature it is reported elsewhere that the photocatalytic decolourization of dyes in aqueous suspension of TiO_2 obeys a Langmuir–Hinshelwood (L–H) kinetic model (Eq. (15)) [13,38]

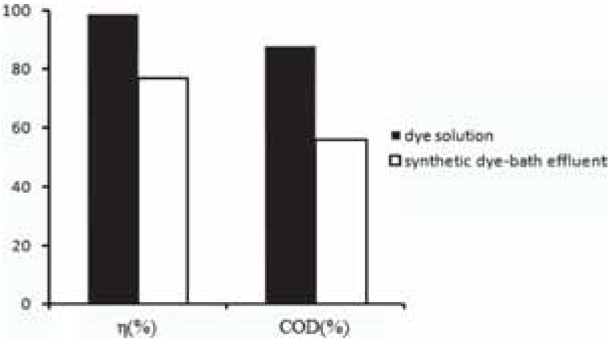

Fig. 6. Decolourization and degradation of synthetic dye-bath effluent. pH = 3, $[TiO_2]$= 2 g L^{-1}, [RO16] = 8.096 × 10^{-2} mM, $\left[S_2O_8^{2-}\right]$=0.5 mM, $[Cu^+]$ =0.5 mM, t = 360 min.

Table 1
COD removal values of synthetic dye-bath effluent and dye solution of RO16

COD (mg/L)	Initial (t = 0)	Final (t = 360 min)	Removal (%)
Synthetic dye-bath effluent	3360	1444	57
Dye solution of RO16	84	19	77

$$r = -\frac{dC}{dt} = \frac{k_r KC}{1 + KC} \tag{15}$$

where r is the decolourization rate of RO16 (mmol L^{-1} min^{-1}), C is concentration of RO16 at time t, k_r reaction rate constant (mmol L^{-1} min^{-1}) and K is the adsorption coefficient of the RO16 onto TiO_2 surface (L $mmol^{-1}$). This model describes that the decolourization rate of RO16 is proportional to the fraction of surface coverage of TiO_2 by dye molecules. It is assumed that dye molecules are strongly adsorbed onto TiO_2 surface rather than intermediates which may interfere by competitive adsorption. In order to minimize this effect, the calculations were made by taken the initial concentrations of RO16. Accordingly, in Eq. (15) the term r can be expressed in terms of r_0 as

$$r_0 = \frac{k_r KC_0}{1 + KC_0} \tag{16}$$

$$\frac{1}{r_0} = \frac{1}{k_r} + \frac{1}{k_r KC_0} \tag{17}$$

where r_0 is the initial decolourization rate of RO16 and C_0 is the initial concentration of RO16. Since the initial dye concentration is low enough (up to 3.238×10^{-2} mM in this study), it is assumed that decolourization rate follows pseudo-first order kinetics and the rate equation is given below by Eq. (18)

$$\ln\left[\frac{C_0}{C}\right] = k_r Kt = k_{app} t \tag{18}$$

To perform L–H kinetics, the decolourization of RO16 was studied over the C_0 range of 8.096×10^{-3}–3.238×10^{-2} mM. Fig. 7 shows linear plots of $\ln(C_0/C)$ versus t with a slope of k_{app}. As can be depicted from data presented in Table 2, a good linearity of $\ln(C_0/C)$ versus t plot was obtained, yielding k_{app} values ranged from 0.018 to 0.010 min^{-1}. A plot of $1/r_0$ versus the $1/C_0$ (Fig. 8) gives a straight line from which k_r and K values were found as 5.862×10^{-4} mmol L^{-1} min^{-1} and 41.22 L $mmol^{-1}$, respectively by the method of least squares ($r^2 = 0.996$). The linear plot of $1/r_0$ versus C_0 indicates that the photocatalytic decolourization of RO16 obeys L–H model.

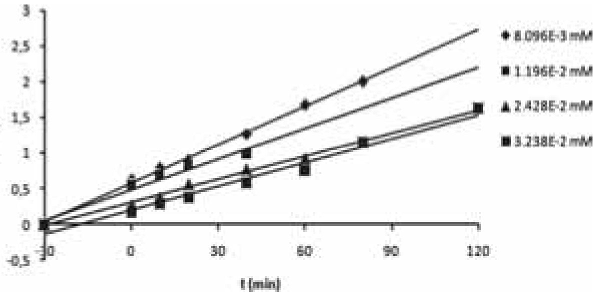

Fig. 7. Kinetics of decolourization of RO16 for different initial concentrations. pH = 3, $[TiO_2]$ = 2 g L^{-1}.

3.5. Solar application of TiO_2 process

Solar energy, which is an abundant natural energy, can be used as an alternative irradiation source in degradation of azo dyes by TiO_2 photocatalysis ($\lambda < 380$ nm), having the possibility of using the solar energy [39]. It is worth to note from Fig. 9 that when the suspension of TiO_2 containing RO16 was exposed to solar irradiation with mean incident sunlight intensity 1.81 mW cm^{-2}, 90% of decolourization and 64% of COD removal were obtained after 120 min of reaction time. However, UV lamp with a mean intensity value of 0.233 mW cm^{-2} yielded 84% of decolourization efficiency and 77% of COD removal under similar experimental conditions. As can be expected, colour is easily removed than COD which requires longer time. The results reveal that solar driven TiO_2 photocatalysis process can be efficiently employed for the decolourization of RO16. The variation of decolourization efficiency with UV lamp power

Table 2
Pseudo-first order kinetic parameter.

C_0 (mM)	Equation	R^2	k_{app} (min^{-1})
8.096×10^{-3}	$y = 0.018x + 0.579$	0.997	0.018
1.619×10^{-2}	$y = 0.015x + 0.486$	0.991	0.015
2.428×10^{-2}	$y = 0.012x + 0.366$	0.996	0.012
3.238×10^{-2}	$y = 0.010x + 0.306$	0.996	0.010

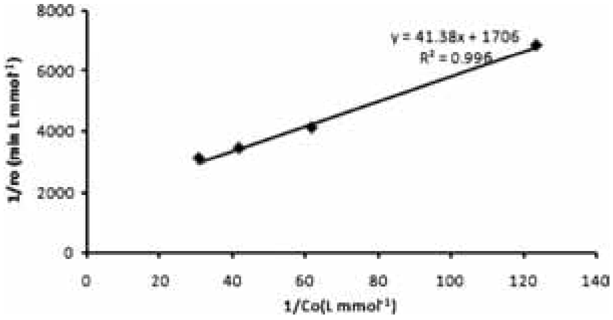

Fig. 8. Variation of reciprocal of initial rate of decolourization of RO16 with reciprocal of initial concentrations. pH = 3, $[TiO_2]$= 2 g L^{-1}.

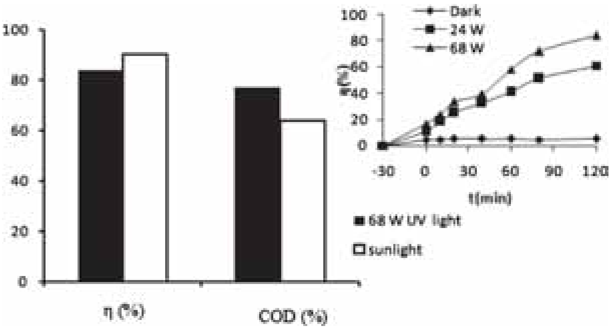

Fig. 9. Effect of solar irradiation on decolourization efficiency and COD removal of RO16. pH = 3, $[TiO_2]$ = 2 g L^{-1}, [RO16] = 8.096 × 10^{-2} mM.

was given in inserted graph in Fig. 9. Increasing UV lamp power from 24 W to 68 W considerably promoted decolourization from 61% to 84%, respectively, due to increased number of photons. In the absence of light TiO_2 powder alone could not promote the decolourization.

3.6. Degradation products

Table 3 reveals the degradation products of RO16 determined by LCMS. The degradation process of RO16 was initiated by OH$^\bullet$ attack to the carbon atom bearing azo-bond chromophore to provide the cleavage of C–N bond which results the formation of compounds containing a naphthalenic ring such as N-(7-dizenyl-8-hydroxy-napthalen-2-yl) acetamide and methyl-naphthalen-2-yl-diazene. These products could undergo oxidation to phthalimide. 4-Oxo-4-phenyl-but-enoic acid and succinic acid are expected to form by further degradation of phthalimide and the remaining part of dye molecule. In the absence of intermediate standards, this is the probable pathway of degradation of RO16 under examined condition. Bilgi and Demir [40] detected the degradation products of RO16 via UV photooxidation by GC/MS and proposed that the first step of degradation is cleavage of azo bond of molecule and naphthalene ring and aromatic and aliphatic acids are formed by successive oxidation of degradation products. Chen [41] identified acetamide as a final product of mineralization of RO16 by GC/MS.

Table 3
Degradation products of RO16. pH = 3, $[TiO_2]$= 2 g L^{-1}, [RO16] = 8.096 × 10^{-2} mM, $\left[S_2O_8^{2-}\right]$ = 0.5mM, $[Cu^+]$ = 0.5 mM.

m/*z*	Compound name	Chemical structure
118	Succinic acid	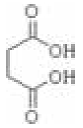
162	Phthalimide	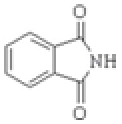
170	Methyl-naphthalen-2-yl-diazene	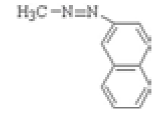
176	4-Oxo-4-phenyl-but-enoic acid	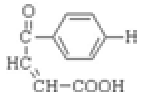
229	N-(7-dizenyl-8-hydroxy-napthalen-2-yl) acetamide	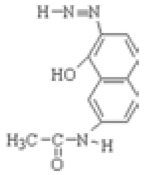

4. Conclusions

In this study, decolourization of C.I. Reactive Orange 16 (RO16) via photocatalysis involving TiO_2/UV and TiO_2/UV/oxidant systems has been investigated. The optimal pH and catalyst concentration values were found to be 3 and 2 g L^{-1}, respectively for TiO_2/UV system. The addition of Cu^+ ions to TiO_2/UV/oxidant system significantly increased the decolourization efficiency. The experimental results reveal that RO16 can be successfully decolourized by TiO_2/UV/$Na_2S_2O_8$/Cu^+ system under irradiation by UV light. The rate of decolourization of RO16 was found to follow pseudo-first order kinetics and obeys L–H model. The applicability of solar light was evaluated and found that solar driven TiO_2 photocatalysis is significantly efficient for the decolourization of RO16. Degradation products of RO16 determined by LCMS were found as N-(7-dizenyl-8-hydroxy-napthalen-2-yl) acetamide, methyl-naphthalen-2-yl-diazene, phthalimide, 4-oxo-4-phenyl-but-enoic acid and succinic acid.

Acknowledgement

The authors would like to thank the Scientific Research Projects Unit of Inonu University for financially supporting this project under BAP grant number 2007/32.

References

[1] C.I. Pearce, J.R. Lloyd and J.T. Guthrie, The removal of color from textile wastewater using whole bacterial cells: a review. Dyes Pigm., 58 (2003) 179–196.

[2] Y. Jiang, Y. Sun, H. Lui, F. Zhu and H. Yin, Solar photocatalytic decolorization of C.I. Basic Blue 41 in an aqueous suspension of TiO_2–ZnO. Dyes Pigm., 78 (2008) 77–83.

[3] M.S. Khehra, H.S. Saini, D.K. Sharma, B.S. Chadha and S.S. Chimni, Biodegradation of azo dye C.I. Acid Red 88 by an anoxic-eaerobic sequential bioreactor. Dyes Pigm., 70 (2006) 1–7.

[4] S. Mondal, Methods of dye removal from dye house effluent – an overview. Environ. Eng. Sci., 25 (2008) 383–396.

[5] Y. Anjaneyulu, N. Sreedhara Chary and D. Samuel Suman Raj, Decolorization of indusrial effluents-available methods and emerging technologies – a review. Rev. Environ. Sci. Bio/Technol., 4 (2005) 245–273.

[6] T. Robinson, G. McMullan, R. Marchant and P. Nigam, Remediation of dyes in texile effluent: a critical review on current treatment technologies with a proposed alternative. Bioresour. Technol., 77 (2001) 247–255.

[7] M.H. Habibi, A. Hassanzadeh and S. Mahdavi, The effect operational parameters on the photocatalytic degradation of three textile azo dyes in aqueous TiO_2 suspensions. J. Photochem. Photobiol. A: Chem., 172 (2005) 89–96.

[8] N. Azbar, T. Yonar and K. Kestioglu, Comparison of various advanced oxidation processes and chemical treatment methods for COD and color removal from a polyester and acetate fiber dyeing effluent. Chemosphere, 55 (2004) 35–43.

[9] Y. Liu, X. Chen, J. Li and C. Burda, Photocatalytic degradation of azo dyes by nitrogen-doped TiO_2 nanocatalysts. Chemosphere, 61 (2005) 11–18.

[10] A. Shafaei, M. Nizakar and M. Arami, Photocatalytic degradation of terephthalic acid using titania and zinc oxide photocatalysts: comparative study. Desalination, 252 (2010) 8–16.

[11] U.G. Akpan and B.H. Hameed, Parameters affecting the photocatalytic of dyes using TiO_2-based photocatalysts: a review. J. Hazard. Mater., 170 (2009) 520–529.

[12] C. Comniellis, A. Kapakla, S. Malato, S.A. Parsons, I. Poulios and D. Mantzavions, Perspective advanced oxidation processes for water treatment: advances and trends for R&D. J. Chem. Technol. Biotechnol., 83 (2008) 769–776.

[13] J. Saien and S. Khezrianjoo, Degradation of the fungicide carbendazim in aqueous solution with UV/TiO_2 process: optimization, kinetics and toxicity studies. J. Hazard. Mater., 157 (2008) 269–276.

[14] M. Kitano, M. Matsuoka, M. Ueshima and M. Anpo, Recent developments in titanium oxide-based photocatalysts. Appl. Catal. A: General, 325 (2007) 1–14.

[15] G. Zayani, L. Bousselmi, P. Pichat and F. Mhenni, A. Ghrabi, Photocatalytic degradation of the acid Blue 113 textile azo dye in aqueous suspensions of four commercialized TiO_2 samples. J. Environ. Sci. Health, Part A, 43 (2008) 202–209.

[16] J. Saien and A.R. Soleymani, Degradation and mineralization of Direct Blue 71 in a circulating upflow reactor by UV/TiO_2 process and employing a new method in kinetic study. J. Hazard. Mater., 144 (2007) 506–512.

[17] C.H. Wu, Effects of operational parameters on the decolorization of C.I. Reactive Red 198 in UV/TiO_2-based systems. Dyes Pigm., 77 (2008) 31–38.

[18] M. Muruganandham and M. Swaminathan, Photocatalytic decolorisation and degradation of Reactive Orange 4 by TiO_2-UV process. Dyes Pigm., 68 (2006) 133–142.

[19] F. Zhang, A. Yediler and X. Liang, Decomposition pathways and reaction intermediate formation of the purified, hydrolyzed azo reactive dye C.I. Reactive Red 120 during ozonation. Chemosphere, 67 (2007) 712–717.

[20] H. Zhang, J. Zhang, F. Liu and D. Zhang, Decolorization of C.I. Acid Orange 52 by ozonation in a hollow fiber membrane. Fresenius Environ. Bull., 18 (2009) 275–279.

[21] T. Kurbus, Y.M. Slokar, A.M. Le Marechal and D.B. Voncina, The use of experimental design for the evaluation of the influence of variables on the H_2O_2/UV treatment of model textile waste water. Dyes Pigm., 58 (2003) 171–178.

[22] K.B. Ko, J.Y. Lee, Y.H. Yoon, T.H. Moon, Y.H. Ahn, C.G. Park, K.S. Min and J.H. Park, Effects of nitrate on the UV photolysis of H_2O_2 for 2,4-dichlorophenol degradation in treated effluents. Desal. Wat. Treat., 2 (2009) 6–11.

[23] S. Papic, D. Vujenic, N. Koprivanac and D. Sinko, Decolorization and mineralization of commercial reactive dyes by using homogeneous and heterogeneous Fenton and UV/Fenton processes. J. Hazard. Mater., 164 (2009) 1137–1145.

[24] J. Feng, X. Hu, P.L. Yue and S. Qiao, Photo Fenton degradation of high concentration Orange II (2 mM) using catalysts containing Fe: A comparative study. Sep. Purif. Technol., 67 (2009) 213–217.

[25] F. Ay, E.C. Catalkaya and F. Kargı, A statistical experiment design approach for advanced oxidation of Direct Red azo-dye by photo-Fenton treatment. J. Hazard. Mater., 162 (2009) 230–236.

[26] Y.H. Huang, Y.F. Huang, P.S. Chang and C.Y. Chen, Comparative study of oxidation of dye-Reactive black B by different advanced oxidation processes: Fenton, electro-Fenton and photo-Fenton. J. Hazard. Mater., 154 (2008) 655–662.

[27] I.K. Konstantinou and T.A. Albanis, TiO_2-assisted photocatalytic degradation of azo dyes in aqueous solution: kinetic and mechanistic investigations – a review. Appl. Catal. B: Environ., 49 (2004) 1–14.

[28] M.I. Litter, Heterogeneous photocatalysis transition metal ions in photocatalytic systems. Appl. Catal. B: Environ., 23 (1999) 89–114.

[29] A. Fujishima, T.N. Rao and D.A. Tryk, Titanium dioxide photocatalysis. J. Photochem. Photobiol. C, 1 (2000) 1–21.

[30] R.S. Juang, S.H. Lin and P.Y. Hsueh, Removal of binary azo dyes from water by UV-irradiated degradation in TiO_2 suspensions. J. Hazard. Mater., 182 (2010) 820–826.

[31] N.M. Mahmoodi, M. Arami and K. Gharanjig, Laboratory studies and COD modeling of photocatalytic degradation of colored textile wastewater by titania nanoparticles. Desal. Wat. Treat., 1 (2009) 312–317.

[32] C.H. Yu, C.H. Wu, T.H. Ho and P.K.A. Hong, Decolorization of C.I. Reactive Black 5 in UV/ TiO_2, UV/oxidant and UV/ TiO_2/oxidant systems: A comparative study. Chem. Eng. J., 158 (2010) 578–583.

[33] K. Soutsas, V. Karayannis, I. Poulios, A. Riga, K. Ntampegliotis, X. Spliotis and G. Papapolymerou, Decolorization and degradation of reactive azo dyes via heterogeneous photocatalytic process. Desalination, 250 (2010) 345–350.

[34] II-H. Cho and K.D. Zoh, Photocatalytic degradation of azo dye (Reactive Red 120) in TiO_2/UV system: optimization and modeling using a response surface methodology (RSM) based on the central composite desing. Dyes Pigm., 75 (2007) 533–543.

[35] M.R. Sohrabi and M. Ghavami, Comparision of Direct Yellow 12 dye degradation efficiency using UV/semiconductor and UV/H_2O_2/semiconductor systems. Desalination, 252 (2010) 157–162.

[36] M.A. Tariq, M. Faisal and M. Muneer, Semiconductor-mediated photocatatalysed degradation of two selected azo dye derivatives, amaranth and bismarck brown in aqueous suspension. J. Hazard. Mater. B,127 (2005) 172–179.

[37] M. Muruganandham and M. Swaminathan, Photochemical oxidation of reactive azo dye with UV–H_2O_2 process. Dyes Pigm., 62 (2004) 269–275.

[38] M. Muruganandham, N. Shobana and M. Swaminathan, Optimization of solar photocatalytic degradation conditions of reactive yellow 14 dye in aqueous TiO_2. J. Mol. Catal. A: Chem., 246 (2006) 154–161.

[39] S. Malato, J. Blanco, A. Vidal, D. Alarcon, M.I. Maldonado, J. Caceres and W. Gernjak, Applied studies in solar photocatalytic detoxification: an overview. Sol. Energy, 75 (2003) 329–336.

[40] S. Bilgi and C. Demir, Identification of photooxidation degradation products of C.I. Reactive Orange 16 dye by gas chromatograpy-mass spectrometry. Dyes Pigm., 66 (2005) 69–76.

[41] C. Chen, Photocatalytic degradation of azo dye Reactive Orange 16 by TiO_2. Water Air Soil Pollut., 202 (2009) 335–342.